Microporous Materials, 1 (1993) 17–32
Elsevier Science Publishers B V, Amsterdam

Study of the geometry and location of the bridging OH groups in aluminosilicate and silicoaluminophosphate type zeolites using ^{1}H MAS NMR sideband analysis and CP/MAS NMR

M Hunger[a,*], M W Anderson[b], A Ojo[b] and H Pfeifer[c]

[a]*Institute of Chemical Technology I, University of Stuttgart, Pfaffenwaldring 55, D-W-7000 Stuttgart 80, Germany*
[b]*Department of Chemistry, UMIST, P O Box 88, Manchester M60 1QD, UK*
[c]*Department of Physics, University of Leipzig, Linnestraße 5, D-O-7010 Leipzig, Germany*

(Received 29 July 1992, accepted 10 September 1992)

Abstract

A numerical analysis of the ^{1}H MAS NMR sideband pattern of the bridging OH groups in various zeolites of the aluminosilicate type (LTA, faujasite, erionite, mordenite, pentasil) and of the silicoaluminophosphate type (SAPO-5, -17, -34, -37) yields H–Al distances of the hydroxyl protons to the adjacent framework aluminium nucleus which cover a range between 0 234 and 0 252 nm From the results, a relation between the H–Al distance and the size of the oxygen rings (6-, 8-, 10- and 12-membered oxygen rings) could be derived Using ^{29}Si CP/MAS NMR it was shown that the bridging OH groups in zeolites of the aluminosilicate type are located at the Si(*n*Al) sites with the largest possible number *n* While the second coordination sphere of the T positions of the bridging OH groups in zeolites of the silicoaluminophosphate type (Si/(Al + P + Si) < 0 12) is occupied by the same number of phosphorus and aluminium atoms, the bridging OH groups in zeolites of the aluminosilicate type with medium framework aluminium densities are located at the Si(*n*Al) sites with $n = 3$, 2 and 1

Keywords zeolite, silicoaluminophosphate, bridging OH group, ^{1}H MAS NMR sideband analysis, geometry

Introduction

Bronsted acid sites play an important role in catalytic reactions which make use of zeolites as catalysts As is well known, bridging OH groups are the source of Bronsted acidity in zeolite catalysts and much attention has been paid to determine their geometry and location Based on *ab initio* quantum-chemical calculations [1–3], values for the atom–atom distances and bond angles of the bridging OH groups in model clusters could be derived (Fig 1) Using neutron powder diffraction on dehydrated faujasites, Czjzek *et al* [4] have determined the structure of the bridging OH groups assuming, however, that there is no difference between the silicon and aluminium atoms By measurement of the second moment M_2 of the ^{1}H broad line NMR signal and a detailed analysis of the various contributions which must be considered, the mean proton–aluminium distance of the bridging OH groups in zeolites of the faujasite and pentasil type has been determined to be $0\,238 \pm 0\,004$ nm [5,6] and $0\,248 \pm 0\,004$ nm [6],

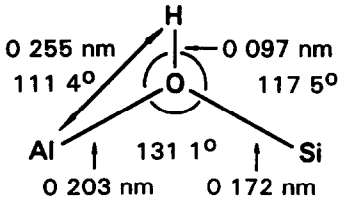

Fig 1 Atom–atom distances and bond angles of a bridging OH group as determined by an *ab initio* quantum-chemical calculation [2]

*Corresponding author

0927–6513/93/$06 00 © 1993 — Elsevier Science Publishers B V All rights reserved

respectively Since in zeolites of the faujasite type two different kinds of bridging OH groups exist, the former value must be assumed to be an average over both these hydroxyl groups In a recent paper [7] a procedure to analyze the ^{1}H MAS NMR sideband pattern of the bridging OH groups in zeolites has been described and successfully applied This new experimental method allows a separate determination of (i) the second moment M_2^{HAl} of the magnetic ^{1}H–^{27}Al interaction and hence of the corresponding distance to the adjacent framework aluminium nucleus r_{HAl}, (ii) the second moment M_2^{ext} of the magnetic dipole interaction of the hydroxyl proton with statistically distributed spins at distances larger than r_{HAl} and (iii) the chemical shift anisotropy $\Delta\sigma_{OH}$ for the various kinds of bridging OH groups in zeolites As typical examples, in ref 7, these quantities have been determined separately for the two kinds of bridging OH groups giving rise to ^{1}H MAS NMR signals at 4 0 and 5 0 ppm in zeolites of the faujasite and SAPO-5 type

The aim of the present paper is to find a relation between the geometry and the location of the bridging OH groups in the zeolite framework ^{1}H MAS NMR measurements were performed at two different magnetic field strengths ($B_0 = 7$ and 9 3 T) in order to prove the consistency of the mathematical model which was used to simulate the ^{1}H MAS NMR sideband pattern From an analysis of ^{29}Si CP/MAS NMR spectra it was possible to derive information concerning the aluminium distribution in the second coordination sphere of the T positions of the bridging OH groups

Experimental

All spectra were recorded with Bruker MSL 300 (^{1}H MAS NMR) and MSL 400 spectrometers (^{1}H, ^{27}Al and ^{29}Si MAS NMR) For the ^{1}H MAS NMR measurements a homemade probe was used to rotate the sealed glass ampoules To eliminate the effects caused by the finite recovery time, for the ^{1}H MAS NMR measurements a $\pi/2$–τ–π–τ pulse sequence was used with a $\pi/2$ pulse length of 3 μs and a pulse delay $\tau = 2\pi/\omega_{rot}$ The MAS frequency $\omega_{rot}/2\pi$ was set to 2000 ± 2 Hz using the automatic Bruker MAS remote control The excitation in the ^{27}Al and ^{29}Si NMR measurements was carried out by $\pi/12$ and $\pi/4$ single pulses, respectively For all ^{1}H MAS NMR and some of the ^{29}Si CP/MAS NMR measurements the samples were calcined in glass ampoules with an inner diameter of 5 5 mm and a batch height of 10 mm The calcination was performed under vacuum with a temperature ramp of 10 K/h At the final temperature of 673 K, the samples were kept for 20 h in a vacuum of 0 01 Pa and sealed off

The zeolites which have been studied are characterized in Table 1 Zeolite A (sample 1), faujasites (samples 2 to 4), erionite (sample 5) and mordenite (sample 6) were prepared from commercial products (Na-A, Na-Y, NaK-erionite and Na-mordenite from CK Bitterfeld) by a NH_4^+ ion-exchange at temperatures of 363 to 393 K, followed by a thermal treatment $25NH_4$Na-A denotes the 25% ammonium exchanged Na-A zeolite The ZSM-5 zeolites (samples 7 and 8) were synthesized according to ref 8 The Na^+/H^+ exchange was carried out with an aqueous solution of 0 05 *N* HCl The zeolite SAPO-5 (sample 9) was synthesized according to ref 9, SAPO-17 and SAPO-34 (samples 10 and 11) according to ref 10 and SAPO-37 (sample 12) was synthesized as described in ref 11

Results

Characterization of the aluminosilicate type zeolites

The ^{29}Si MAS NMR spectrum of the $25NH_4$Na-A zeolite shows one narrow line at $-89\,2 \pm 0\,2$ ppm (Fig 2a) which corresponds to the chemical shift of the Si(4Al) sites in Na-A zeolites (−89 6 ppm [12]) After calcination at 670 K this line is broadened and shifted to −90 2 ppm (Fig 2b) The weak low-field shoulder at $-89\,5 \pm 0\,2$ ppm has to be explained by Si(4Al) sites with sodium cations By cross-polarization (CP/MAS NMR) with mixing times of 2 ms (Fig 2c) and 5 ms the line at −90 2 ppm could be enhanced while the shoulder at −89 5 ppm disappeared In the ^{27}Al MAS NMR spectrum of the calcined and rehydrated 25HNa-A zeolite (Fig 3a),

TABLE 1

Structure data and framework composition of the aluminosilicates and silicoaluminophosphates studied

No	Sample	Structure type	Si/Al[a] Si/(Al+P+Si)[b]	Type and size (nm) of O-rings [25,39,40]
1	25HNa-A	LTA	1.0[a]	8-membered, 0.41
2	50HNa-X	FAU	1.4[a]	12-membered, 0.74 6-membered, 0.25
3	52HNa-Y	FAU	2.6[a]	[c]
4	90HNa-Y	FAU	3.5[a]	[c]
5	37HNaK-ERI	ERI	2.9[a]	8-membered, 0.36 × 0.51
6	H-M	MOR	7.1[a]	12-membered, 0.65 × 0.70 8-membered, 0.26 × 0.57
7	H-ZSM-5/1	MFI	15.0[a]	10-membered, 0.53 × 0.56 0.51 × 0.55
8	H-ZSM-5/2	MFI	26.0[a]	[d]
9	SAPO-5	AFI	0.036[b]	12-membered, 0.73 6-membered, 0.25
10	SAPO-17	ERI	0.021[b]	8-membered, 0.36 × 0.51
11	SAPO-34	CHA	0.114[b]	8-membered, 0.38
12	SAPO-37	FAU	0.121[b]	12-membered, 0.74 6-membered, 0.25

[a]Framework Si/Al ratio determined by ^{29}Si MAS NMR [b]Mole fraction Si/(Al+P+Si) of silicoaluminophosphates [c]As sample 2 [d]As sample 7

TABLE 2

^{1}H MAS NMR chemical shifts and IR wave numbers of bridging OH groups of the zeolites studied

No	Sample	Chemical shift (ppm)	IR wave number (cm^{-1})
1	25HNa-A	4.0 [18]	3620 [18]
2	50HNa-X	3.8 [18]	3658 [18]
3	52HNa-Y	3.9	3645 [18]
4	90HNa-Y	3.9	3647
		5.0 [18]	3565 [20]
5	37HNaK-ERI	3.9 [28]	3618 [20,27]
6	H-M	4.2 [18]	3610 [18,20]
7	H-ZSM-5/1	4.2 [14]	3610 [18]
8	H-ZSM-5/1	4.2 [14]	3620 [18]
9	SAPO-5	3.8	3625
		4.8 [30]	3520 [30]
10	SAPO-17	3.7	3615–3624
		4.0	3591
		4.8 [34]	3525 [34]
11	SAPO-34	3.8 [30]	3600–3625 [30]
12	SAPO-37	3.8	3639
		4.3	3572 [11,35]

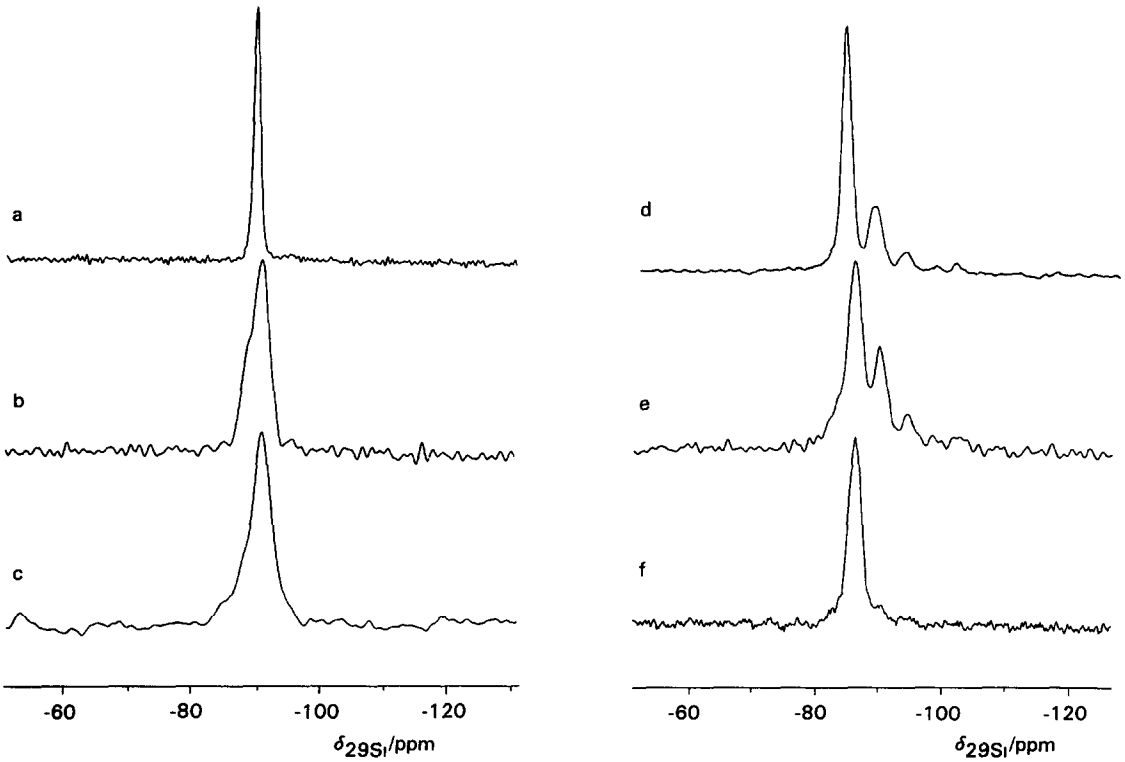

Fig 2 ^{29}Si MAS NMR spectra of the hydrated 25NH_4Na-A (a), the calcined 25HNa-A recorded without (b) and with CP (c), the hydrated 50NH_4Na-X (d) and the calcined 50HNa-X recorded without (e) and with CP (f)

besides the signal of tetrahedrally coordinated framework aluminium at 58 6±1 0 ppm, only a weak signal at 0 0±1 0 ppm was observed The latter line is caused by a small amount of octahedrally coordinated extra-framework aluminium The ^{1}H MAS NMR spectrum of the calcined 25HNa-A zeolite (Fig 4a) consists of three signals with chemical shifts of 0 5±0 1, 2 0±0 1 and 4 0±0 1 ppm According to the references in Table 2 the line at 4 0 ppm is caused by the bridging OH groups which undergo a heteronuclear interaction with the adjacent framework aluminium nuclei (^{1}H MAS NMR sideband pattern) The line at 2 0 ppm is due to the SiOH groups at the outer surface, at the lattice defects or in amorphous phases [14,15] By an X-ray diffraction study of the NaA zeolite, $[Al(OH)_4]^-$ species were found at the extra-framework positions [13] In the ^{1}H MAS NMR spectra of α-Al_2O_3 a line at −0 2 ppm was interpreted by $[AlOH]^{2+}$ groups at the outer surface of the particles [16], and in the case of MgNa-Y zeolites a line due to metal OH groups appears at about 0 ppm [17] Considering these values, the ^{1}H NMR line at 0 5 ppm may be explained by a small amount of aluminium OH species at extra-framework positions

The ^{29}Si MAS NMR spectrum of the hydrated 50NH_4Na-X zeolite (Fig 2d) consists of lines with chemical shifts of −84 2±0 2, −88 9±0 2 and −94 1±0 2 ppm caused by the silicon atoms at the Si(4Al), Si(3Al) and Si(2Al) sites [12], respectively In the spectrum of the calcined 50HNa-X zeolite (Fig 2e) these lines are broadened and shifted slightly to higher magnetic field Moreover, the intensities of the lines of Si(3Al) and Si(2Al) at −91 0±0 2 and −95 7±0 2 ppm, respectively, were increased relative to the spectrum in Fig 2d The framework Si/Al ratio, determined from these spectra amounts to 1 2 before and to 1 4 after the calcination In the ^{29}Si CP/MAS NMR spectra with mixing times of 2 ms (Fig 2f) and 5 ms only the line of the Si(4Al) sites at −87 3±0 2 ppm is

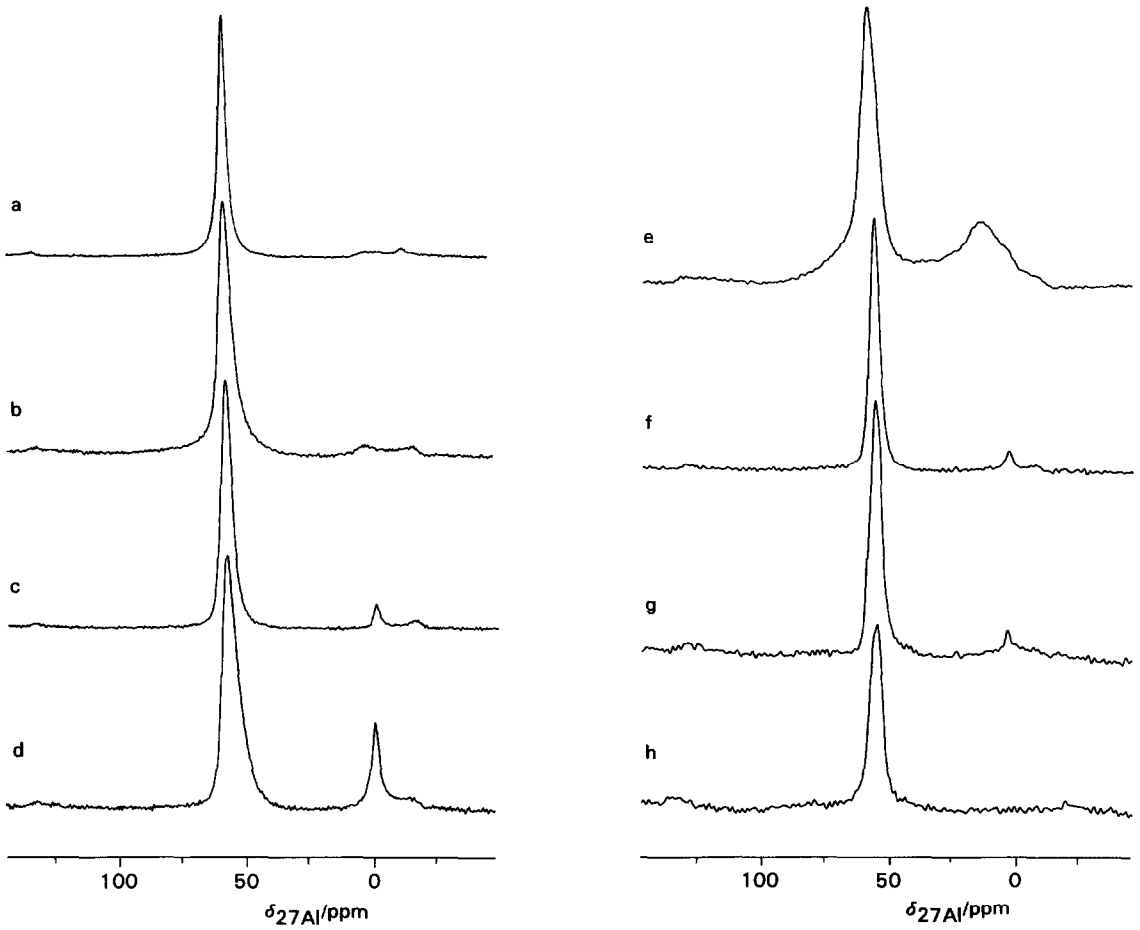

Fig 3 ^{27}Al MAS NMR spectra of the calcined and rehydrated 25HNa-A (a), 50HNa-X (b), 52HNa-Y (c), 90HNa-Y (d), 37HNaK-ERI (e), H-mordenite (f), H-ZSM-5/1 (g) and H-ZSM-5/2 (h)

enhanced while all other lines disappear In agreement with the above-mentioned weak dealumination, the ^{27}Al MAS NMR spectrum of the calcined and rehydrated 50HNa-X zeolite (Fig 3b) exhibits only a small line of octahedral extra-framework aluminium at $0\,0\pm1\,0$ ppm The ^{1}H MAS NMR spectrum of the calcined 50HNa-X zeolite consists of a line of bridging OH groups at $3\,9\pm0\,1$ ppm with a strong ^{1}H MAS NMR side-band pattern (Fig 4b) As shown below for zeolite Y, this signal corresponds to the bridging hydroxyl protons in the large cavities of the faujasite structure

The ^{29}Si MAS NMR spectra of the calcined 52HNa-Y and 90HNa-Y zeolite (Figs 5b and 5e) show a strong broadening of all lines relative to those of the hydrated $52NH_4$Na-Y and $90NH_4$Na-Y zeolites (Figs 5a and 5d) observed at $-90\,3\pm0\,2$, $-95\,3\pm0\,2$, $-101\,1\pm0\,2$ and $-105\,5\pm0\,2$ ppm According to the intensity ratio of the Si(nAl) sites ($n=3$, 2, 1, 0), the calcination causes only a weak dealumination for the $52NH_4$Na-Y zeolite while for the $90NH_4$Na-Y zeolite the framework Si/Al ratio increases from 2 6 to 3 4 The shapes of the ^{29}Si CP/MAS NMR spectra of the calcined 52HNa-Y and 90HNa-Y zeolites (Figs 5c and 5f) correspond to those in Figs 5b and 5c, caused by a small amount of Si(3Al) sites at $-91\,5\pm0\,5$ ppm (52HNa-Y), Si(2Al) sites at $-96\,1\pm0\,2$ ppm and Si(1Al) sites at $-101\,4\pm0\,2$ ppm, and a weak

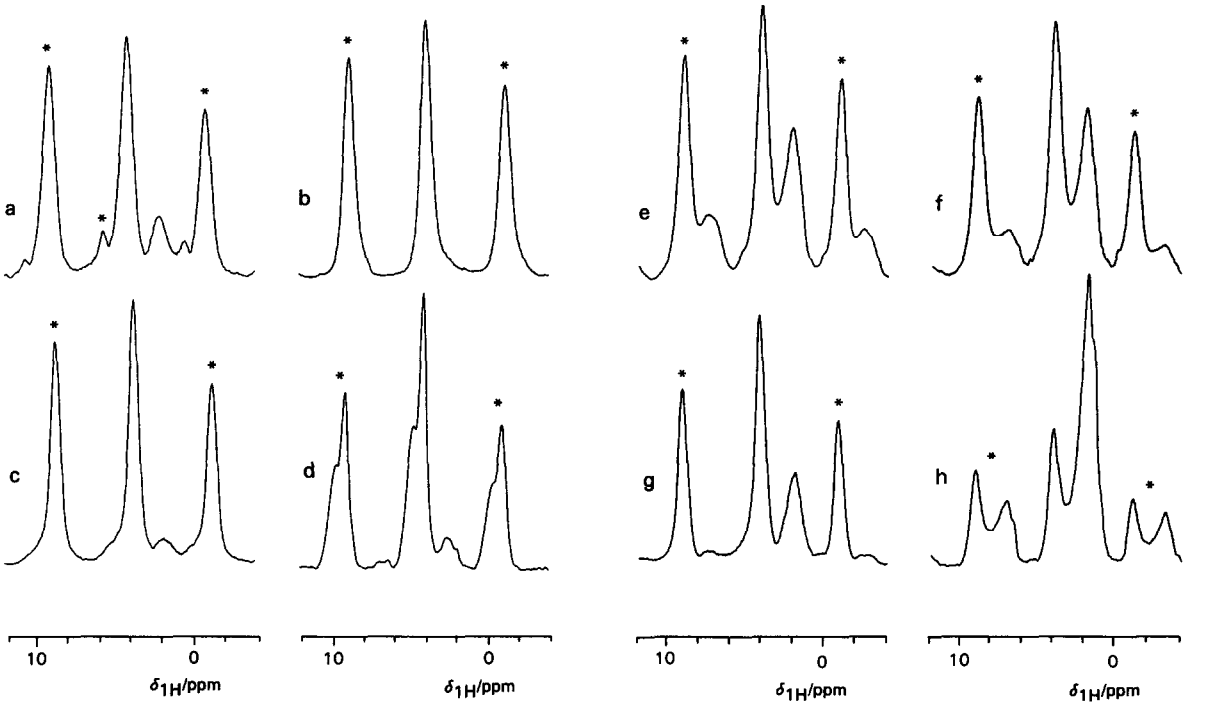

Fig 4 Central line and first sidebands (*) of the ^{1}H MAS NMR spectra of calcined 25HNa-A (a), 50HNa-X (b), 52HNa-Y (c), 90HNa-Y (d), 37HNaK-ERI (e), H-M (f), HZSM-5/1 (g) and HZSM-5/2 (h)

shoulder of Si(0Al) sites at -105.5 ± 0.2 ppm As a result of the above-mentioned dealumination, the ^{27}Al MAS NMR spectra of the calcined and rehydrated 52HNa-Y and 90NH_4Na-Y zeolites (Figs 3e and 3f) show signals of octahedrally coordinated extra-framework aluminium at 0.0 ± 1.0 ppm The ^{1}H MAS NMR spectra of the 52HNa-Y and the 90HNa-Y zeolites (Figs 4c and 4d) consist of signals with a chemical shift of 1.8 ± 0.1, 3.9 ± 0.1 and 5.0 ± 0.2 ppm ^{1}H MAS NMR studies [18,19] on 36, 64 and 90% decationized faujasites have yielded lines of SiOH groups with a chemical shift of 1.8 ppm and two lines with 3.9 and 5.0 ppm which are due to the bridging OH groups in the large cavities and the hexagonal prisms of the sodalite cages, respectively The latter two signals correspond to the well-known HF and LF bands in IR spectroscopy with wave numbers of 3647 and 3565 cm^{-1} [20], respectively In agreement with this correlation, after adsorption of perdeuterated pyridine the bridging OH groups at 4.0 ppm are at first involved in the protonation of the adsorbed base This protonation gives rise to a broad line of pyridinium ions with a ^{1}H NMR chemical shift of 16.0 ± 1.0 ppm [14,22] As shown by IR studies on faujasites [21], at a sodium exchange degree of 52% there is only a small amount (<5%) of bridging OH groups located in the hexagonal prisms of the sodalite cages causing the small shoulder at about 5 ppm (Fig 4c).

Because of the different ^{29}Si NMR chemical shifts of the silicon atoms at the crystallographically non-equivalent T1 and T2 sites in the erionite structure [12,23,24], the determination of the framework Si/Al ratio requires assumptions concerning the aluminium distribution The ^{29}Si MAS NMR spectrum of the hydrated 37NH_4NaK-erionite (Fig 5g), which consists of lines with a chemical shift of -96.6 ± 0.2, -101.3 ± 0.2 and -105.9 ± 0.2 ppm, and weak shoulders at -92.5 ± 0.4 and

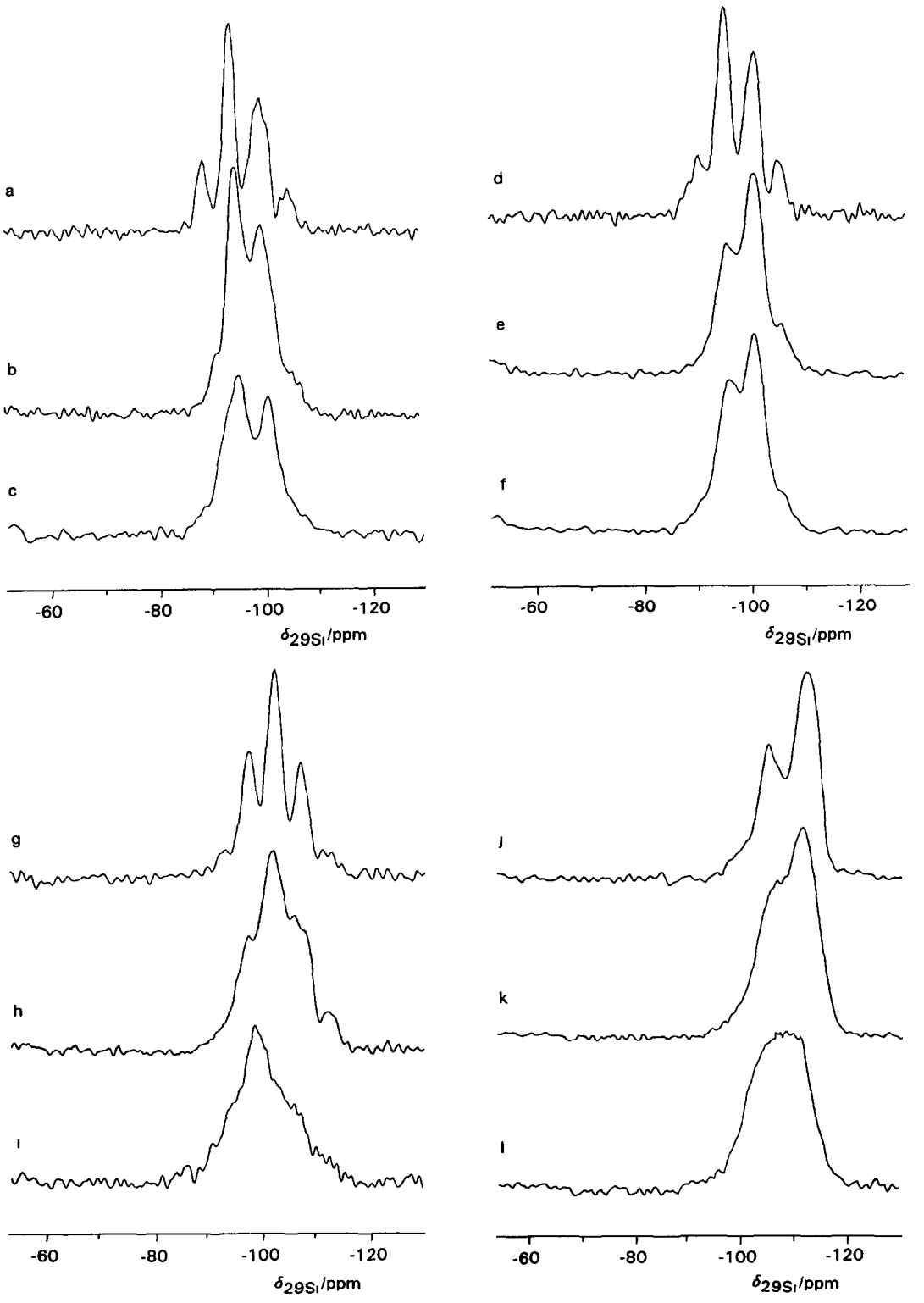

Fig 5 ^{29}Si MAS NMR spectra of the hydrated $52NH_4Na$-Y (a), the calcined 52HNa-Y recorded without (b) and with CP (c), the hydrated $90NH_4Na$-Y (d), the calcined 90HNa-Y recorded without (e) and with CP (f), the hydrated $37NH_4NaK$-erionite (g) and the calcined 37HNaK-ERI recorded without (h) and with CP (i), the hydrated H-mordenite (j) and the calcined H-mordenite recorded without (k) and with CP (l)

−111 1±0 4 ppm, agrees very well with that of a synthetic erionite with a framework Si/Al ratio of 2 6 and a $(Si/Al)_{T1}$-to-$(Si/Al)_{T2}$ ratio of 0 5 [23] The calcination of this sample at 673 K causes a broadening of all ^{29}Si NMR lines and a slight shift to a higher magnetic field (Fig 5h) while the intensity ratio of all lines seems to be the same as before The weak signal at −103 5±0 5 ppm is due to silanol groups at the defects of the zeolite framework [12] The ^{29}Si CP/MAS NMR spectrum of the calcined 37HNaK-erionite (Fig 5i) consists of a broad line with a peak maximum at −98 4±0 2 ppm corresponding to the signal of $Si_{T1}(2Al)+Si_{T2}(3Al)$ [12], high-field shoulders of $Si_{T1}(1Al)+Si_{T2}(2Al)$ at about −102 ppm and silanol groups at about −103 5 ppm In the ^{27}Al MAS NMR spectrum of the calcined and rehydrated 37HNaK-erionite (Fig 3e), besides the signal of tetrahedrally coordinated framework aluminium, a strong line at 10 0±1 0 ppm appears It is well known that the synthesis of erionite is normally accompanied by the formation of other aluminosilicates X-ray studies on the parent NaK-erionite have shown a contribution of zeolite P [26] which is thermally unstable in the H-form and responsible for extra-framework aluminium and amorphous SiO_2 in the calcined sample The ^1H MAS NMR spectrum of the 37HNaK-erionite consists of lines with a chemical shift of 2 0±0 1 and 3 9±0 1 ppm (Fig 4e) Contrary to all other samples, the ^1H NMR line at 2 0 ppm shows a MAS NMR sideband pattern which is characteristic for hydroxyl protons under the influence of a heteronuclear magnetic dipole interaction Hence, aluminium OH groups at extra-framework aluminium species which are formed during the thermal decomposition of zeolite P may contribute to the line at 2 0 ppm IR studies of 35HNaK-erionites have yielded IR bands at 3618 cm^{-1} for bridging OH groups [26] and at 2670 cm^{-1} for bridging OD groups [28,29] It could be shown [29] that these hydroxyl groups can be removed by Cs exchange, so that they were attributed to OH groups located in the erionite cages Only for cation exchange degrees exceeding 47%, a second type of bridging OH groups at 3566 cm^{-1} could be observed [26] Hence, one has to conclude that in the 37HNaK-erionite the bridging OH groups exhibiting a ^1H NMR chemical shift of 3 9 ppm are caused by O1H groups located in the 8-membered oxygen rings of the erionite cages

The ^{29}Si MAS NMR spectra of the hydrated mordenite (Fig 5j) and H-ZSM-5 zeolites (not shown) consist of two lines with chemical shifts of −105 5±0 2 and −111 8±0 2 ppm corresponding to the silicon atoms at the Si(1Al) and Si(0Al) sites As shown in Fig 5k the calcination of these samples causes a broadening and a shift of the Si(1Al) line by about 3 ppm to higher magnetic field The calcination did not change the intensity ratio of the Si(1Al) and Si(0Al) sites By cross-polarization (Fig 5l) the intensity of the broad line of the Si(1Al) sites with a chemical shift of −108 0±1 0 ppm is enhanced According to the high thermal stability of these zeolites, in the ^{27}Al MAS NMR spectra of the calcined and rehydrated samples weak (Figs 3f and 3g) or no (Fig 3h) signals of octahedrally coordinated extra-framework aluminium near 0 ppm were observed The ^1H MAS NMR spectra of the H-mordenite and H-ZSM-5 zeolites (Figs 4f, 4g and 4h) comprise lines of SiOH groups at 2 0±0 1 ppm and bridging OH groups at 4 2±0 1 ppm In earlier papers [14,22] it was shown that after adsorption of perdeuterated pyridine, the OH groups at 4 2 ppm disappear as a result of the protonation of pyridine to pyridinium ions Hence, the bridging hydroxyl protons with a ^1H NMR chemical shift of 4 2 ppm are located in the 10- and 12-membered oxygen rings of the ZSM-5 and mordenite channel system, respectively

Characterization of the silicoaluminophosphate type zeolites

The ^{29}Si MAS NMR spectra of the silicoaluminophosphates consist of lines with chemical shifts of −89 5±0 2 (SAPO-34 and SAPO-37), −93 5±0 2 (SAPO-5), −93 1±0 2 (SAPO-17) and −97 4±0 2 ppm (SAPO-17), corresponding to incorporation of silicon atoms into the aluminophosphate framework at the phosphorous positions causing Si(4Al) sites (Figs 6a and 6c–6e) The splitting of the latter two lines is caused by the Si(4Al) sites at the crystallographically non-equivalent T1 and T2 positions, respectively, in the

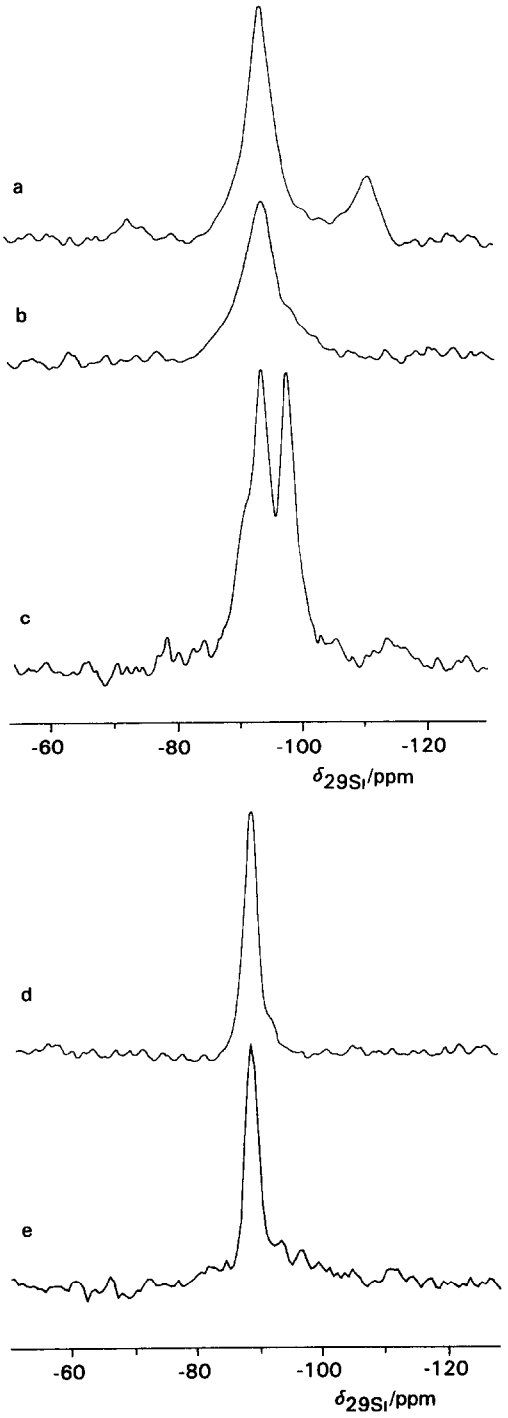

Fig 6 ^{29}Si MAS NMR spectra of the calcined SAPO-5 recorded without (a) and with CP (b) and of the hydrated SAPO-17 (c), SAPO-34 (d) and SAPO-37 (e)

erionite structure of the SAPO-17 molecular sieve The signal at $-109\,5\pm0\,2$ ppm, observed in the spectrum of SAPO-5 (Fig 6a) is due to the Si(4Si) sites To compensate the negative charge of the framework, bridging OH groups were formed in the neighbourhood of the Si(4Al) sites In agreement with this interpretation, in the ^{29}Si CP/MAS NMR spectrum of the calcined SAPO-5 (Fig 6b) the line of the Si(4Al) sites with a chemical shift of $-93\,5\pm0\,2$ ppm is enhanced

In earlier papers [30,31] the ^{1}H NMR lines at $1\,5\pm0\,1$, $3\,8\pm0\,1$ and $4\,8\pm0\,1$ ppm, observed in the spectra of SAPO-5 (Fig 7a), were attributed to silanol groups and two kinds of bridging OH groups It was shown that after adsorption of perdeuterated cyclohexane (diameter of 0 6 nm [25]) the line at 3 8 ppm disappears due to the deuteron exchange with the hydroxyl protons in the large channels [30] After 10 days the intensity

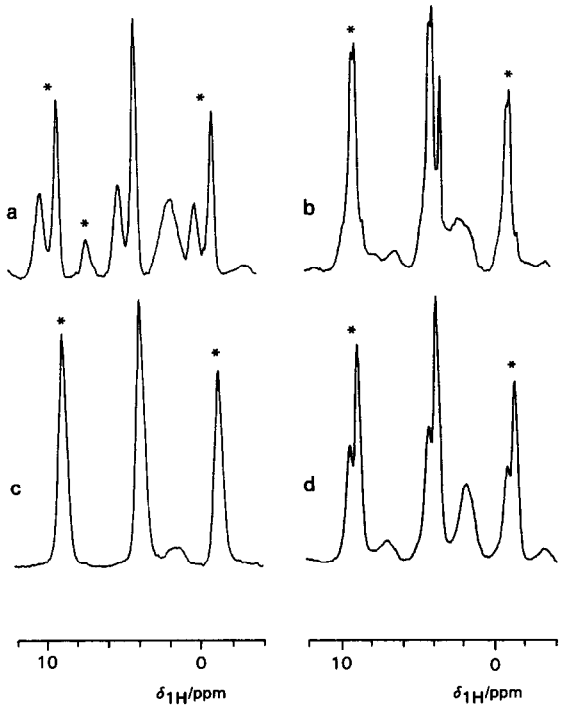

Fig 7 Central line and first sidebands (*) of the ^{1}H MAS NMR spectra of the SAPO-5 (a), SAPO-17 (b), SAPO-34 (c) and SAPO-37 (d)

of the signal at 4 8 ppm has decreased dramatically as a result of deuteron exchange among all bridging OH groups while the line at 1 5 ppm remained unaffected as before Hence, the ^{1}H NMR line at 3 8 ppm was attributed to the bridging OH groups in the 12-membered oxygen rings of the channels and the line at 4 8 ppm to the non-accessible bridging OH groups in the 6-membered oxygen rings

The ^{1}H MAS NMR spectrum of the erionite type SAPO-17 comprises lines at chemical shifts of $1\,5\pm0\,1$, $3\,2\pm0\,1$, $3\,7\pm0\,1$ and $4\,0\pm0\,1$ ppm, and a weak shoulder at $4\,8\pm0\,1$ ppm (Fig 7b) While the former two of these signals are due to the SiOH and POH [33] groups at the lattice defects or at the outer surface, the latter three signals with strong MAS NMR sideband pattern are caused by the bridging OH groups As a result of a combined NMR and IR study of SAPO-17 [34], the signals at 3 7 and 4 0 ppm were proposed to be attributable to the bridging OH groups in the neighbourhood of the $Si_{T2}(4Al)$ and $Si_{T1}(4Al)$ sites, respectively, *i e*, of silicon atoms incorporated in the $AlPO_4$-17 framework at the T2 ($\delta_{^{29}Si} = -97\,4$ ppm) and T1 ($\delta_{^{29}Si} = -93\,1$ ppm) positions The corresponding IR bands of these bridging OH groups appear at 3615 to 3624 and 3591 cm^{-1}, respectively Both kinds of bridging OH groups are accessible for probe molecules as could be shown by adsorption of *n*-hexane Hence, the hydroxyl protons with a ^{1}H NMR chemical shift of 3 7 ppm as well as those at 4 0 ppm must be located in the 8-membered oxygen rings of the zeolite framework Since the low-field shoulder (< 5% of the total intensity) has the same chemical shift as the low-field signal in SAPO-5 (4 8 ppm), these OH groups were attributed to the bridging hydroxyl protons located in the 6-membered oxygen rings of the cancrinite units

The ^{1}H MAS NMR spectrum of the chabazite type SAPO-34 consists of two lines at $1\,5\pm0\,1$ and $3\,8\pm0\,1$ ppm (Fig 7c) which are due to SiOH and bridging OH groups, respectively While after adsorption of perdeuterated pyridine no interaction with the bridging hydroxyl protons was observed, a reammoniation of the calcined SAPO-34 leads to a disappearence of the line at 3 8 ppm and to the appearence of the signal of ammonium ions at 6 8 ppm [30] Contrary to the ammonia molecules (diameter of 0 26 nm [25]), the pyridine molecules are too large (diameter of about 0 58 nm [25]) to enter the 8-membered oxygen rings of the chabazite structure where the bridging OH groups are located

The ^{1}H MAS NMR spectrum of the faujasite type SAPO-37 comprises three lines at $1\,6\pm0\,1$, $3\,8\pm0\,1$ and $4\,3\pm0\,1$ ppm (Fig 7d) corresponding to IR bands at 3746, 3639 and 3572 cm^{-1} [11,35], respectively Dzwigaj *et al* [35] have shown that after adsorption of pyridine the hydroxyl protons of the latter two IR bands behave like the bridging OH groups in the large cavities and in the sodalite cages of the faujasite structure, respectively Hence, the ^{1}H NMR lines at 3 7 and 4 2 ppm were also attributed to the bridging OH groups in the 12-membered oxygen rings of the large cavities and the 6-membered oxygen rings of the hexagonal prisms of the sodalite cages It is interesting to note that both the ^{1}H NMR low-field line (4 2 ppm) as well as the IR low-frequency band (3572 cm^{-1}) appear at distinctly different positions than in the faujasite type aluminosilicate

Discussion

MAS sideband analysis

To simulate the ^{1}H MAS NMR sideband pattern of the bridging OH groups, the envelope of the free induction decay has been described by the following equation [7]

$$G(t) = G^{ext}(t) \ll \exp\{-\int_0^t \omega(t)\,dt\} >_{powder} >_m \qquad (1)$$

The frequency function

$$\omega(t) = \mathbf{b}(t)\,[\mathbf{T}(\Delta\sigma_{OH}) + m\,\mathbf{T}(M_2^{HAl})]\,\mathbf{b}^T(t) \qquad (2)$$

is defined as the difference between the resonance frequency of a bridging OH group fixed in one of the various orientations and the resonance frequency for the isotropic value of the chemical shift The latter corresponds to the situation of a fast isotropic reorientation so that the chemical shift becomes isotropic and the magnetic dipole interaction is averaged to zero $\mathbf{b}(t)$ denotes the unit

vector along the direction of the static magnetic field in the bridging OH group system, which becomes a periodic function of time under MAS conditions $\mathbf{T}(\Delta\sigma_{OH})$ is the traceless tensor of the chemical shift anisotropy $\Delta\sigma_{OH}$, m is the magnetic spin quantum number of the S spins (framework aluminium) and $\mathbf{T}(M_2^{HAl})$ denotes the traceless tensor of the magnetic dipole interaction between the hydroxyl proton and the adjacent framework aluminium nucleus The distance r_{HAl} between both may be calculated in nm from the second moment M_2^{HAl} determined in s^{-2} by

$$r_{HAl}=(90\,24\cdot 10^3/M_2^{HAl})^{1/6} \quad (3)$$

The factor

$$G^{ext}(t)=\exp\{-(M_2^{ext}/\omega_{rot}^2)\,[(2/3)(1-\cos(\omega_{rot}t) + (1/12)(1-\cos(2\omega_{rot}t))]\} \quad (4)$$

accounts for the magnetic dipole interactions between a bridging hydroxyl proton and the nuclei which are statistically distributed at distances larger than r_{HAl} M_2^{ext} denotes the corresponding second moment and ω_{rot} the MAS angular frequency For a numerical analysis of experimentally recorded ^{1}H MAS NMR sideband spectra, the intensities of the sideband pattern were calculated using eqn (1) The asymmetry of the chemical shift tensor was assumed to be zero, which seems to be justified by an inspection of data for related systems [37,38] Finally, the intensities of the first five experimentally recorded MAS sidebands were fitted to the calculated sideband pattern by minimizing the normalized quadratic deviation with respect to the values of M_2^{HAl}, M_2^{ext} and $\Delta\sigma_{OH}$ A more detailed description of the MAS NMR sideband analysis of bridging OH groups in zeolites was published previously [7]

^{1}H MAS NMR sideband pattern recorded at different B_0-fields

In Table 3 the values for r_{HAl}, $\Delta\sigma_{OH}$ and M_2^{ext} are collected which were determined numerically by MAS sideband analysis of the ^{1}H MAS NMR spectra of the bridging OH groups in the zeolites under study While the sideband intensities caused by the heteronuclear magnetic dipole interaction do not depend on the strength of the applied magnetic field, the chemical shift anisotropy is proportional to the field strength Hence, the MAS sideband pattern of bridging hydroxyl protons with $\Delta\sigma_{OH}=14\,5\pm2\,0$ ppm exhibit different sideband intensities in the spectra recorded at $B_0=7$ and 9 4 T (compare Figs 8a and 8b) If the mathematical model and the assumptions used for the MAS sideband simulation are correct, the minimum of the normalized quadratic deviation between the simulated and the experimentally recorded spectra measured at $B_0=7$ and 9 4 T must yield the same values for M_2^{HAl}, $\Delta\sigma_{OH}$ (in the ppm scale) and M_2^{ext} As can be seen from Table 3, the anisotropies of the chemical shift of the samples 3, 7 and 11, determined at proton resonance frequencies of 300 MHz and 400 MHz, agree very well considering an accuracy of $\pm2\,0$ ppm Inserting the value of the second moment M_2^{HAl} of the heteronuclear ^{1}H–^{27}Al interaction into eqn (3), the H–Al distance between the hydroxyl protons and the adjacent framework aluminium nucleus has been calculated Also, as it should be these values do not depend on the magnetic field strength B_0 within the accuracy of $\pm0\,002$ nm

H–Al distances determined by ^{1}H MAS NMR sideband analysis

As has been shown previously [7], the H–Al distance of the bridging OH groups in the 6-membered oxygen rings of the HNa-Y zeolite is about 0 015 nm smaller than the H–Al distance of the bridging OH groups in the 12-membered oxygen rings The ^{1}H MAS NMR sideband analysis of the faujasite type SAPO-37 and the AFI type SAPO-5 has confirmed this relation (samples 9 and 12 in Table 3 and Figs 8c and 8d) For the OH groups in the large cavities and the hexagonal prisms of the faujasites, Olson and Dempsey [36] proposed a location of the hydroxyl protons at the O1 and O3 bridges, respectively By *ab initio* quantum-chemical calculations Schroder *et al* [3] have derived geometrical data for the Si–O1H–Al and Si–O3H–Al clusters which correspond to the bridging OH groups located in the large and small cavities of the faujasite structure, respectively Their

TABLE 3

Results of an analysis of the ^{1}H MAS NMR sideband pattern of bridging OH groups of the zeolites studied[a]

No	Sample	Line (ppm)	Reson freq (MHz)	M_2^{HAl} (10^8 s^{-2})	M_2^{ext} (10^8 s^{-2})	r_{HAl} (nm)	$\Delta\sigma_{OH}$ (ppm)
1	25HNa-A	4 0	400	4 97	1 24	0 238	14 5
2	50HNa-X	3 9	400	4 07	1 42	0 246	14 0
3	52HNa-Y	3 9	300	3 52	0 83	0 252	14 0
			400	3 70	1 05	0 250	15 0
4	90HNa-Y	3 9	400	3 70	1 22	0 250	16 0
		5 0	400	5 23	0 86	0 236	16 5
5	37HNaK-ERI	3 9	400	4 07	1 54	0 246	14 0
6	H-M	4 2	400	3 88	0 53	0 248	14 0
7	H-ZSM-5/1	4 2	300	3 70	0 29	0 250	15 5
			400	3 70	0 51	0 250	13 5
8	H-ZSM-5/2	4 2	400	4 07	0 20	0 246	15 5
9	SAPO-5	3 8	400	3 52	0 94	0 252	15 0
		4 8	400	5 23	1 18	0 236	17 5
10	SAPO-17	3 7	400	4 49	1 18	0 242	14 5
		4 0	400	4 72	1 06	0 240	16 0
11	SAPO-34	3 8	300	4 28	0 92	0 244	14 5
			400	4 49	1 28	0 242	13 5
12	SAPO-37	3 8	400	3 70	1 12	0 250	14 0
		4 3	400	5 50	1 34	0 234	15 0

[a]The mean errors are $\pm 0\,2\ 10^8$ s^2 for the second moments M_2^{HAl} and M_2^{ext}, $\pm 0\,002$ nm for the proton–aluminium distance r_{HAl} and $\pm 2\,0$ ppm for the anisotropy of the chemical shift $\Delta\sigma_{OH}$

results for the H–Al distances are 0 239 and 0 233 nm, respectively Although there is no quantitative agreement between the theoretical H–Al distances of the O1H and O3H groups and the experimentally determined r_{HAl} values (compare r_{HAl} in Table 3), both methods reveal the same result the hydroxyl protons of the bridging OH groups in the 6-membered oxygen rings have a smaller distance to the adjacent framework aluminium nuclei than those in the 12-membered oxygen rings

In Fig 9a the H–Al distances r_{HAl} (Table 3) of all samples under study are plotted as a function of the number of oxygen atoms per oxygen ring Although there are differences in the r_{HAl} values of up to 0 004 nm for the bridging hydroxyl protons located in the same oxygen ring type, a correlation becomes apparent between the H–Al distance and the location of the bridging hydroxyl protons in the 6-, 8-, 10- and 12-membered oxygen rings Using the mean diameter ϕ_O of each type of oxygen ring and the mean value r_{HAl} of the hydroxyl protons located in these oxygen rings (Tables 1 and 3), the following equation can be found by linear regression (see also Fig 9b)

$$r_{HAl}/\text{nm} = 0\,035\ \phi_O/\text{nm} + 0\,227 \quad (5)$$

The corresponding correlation coefficient R is 0 9386 Hence, the determination of the H–Al distance r_{HAl} for a bridging hydroxyl group allows an estimate of the size of the oxygen ring ϕ_O to which the hydroxyl proton is attached by the inverse of eqn (5)

$$\phi_O/\text{nm} = 28\,6\ r_{HAl}/\text{nm} - 6\,5 \quad (6)$$

Characterization of the atoms in the second coordination sphere of the T positions

In the ^{29}Si CP/MAS NMR experiments using calcined zeolites, the magnetization transfer takes place from the hydroxyl protons to the adjacent ^{29}Si spins Since for the samples under study a splitting of the ^{1}H NMR lines of the bridging OH groups of up to 1 ppm was observed, the residence time of these hydroxyl protons at the framework

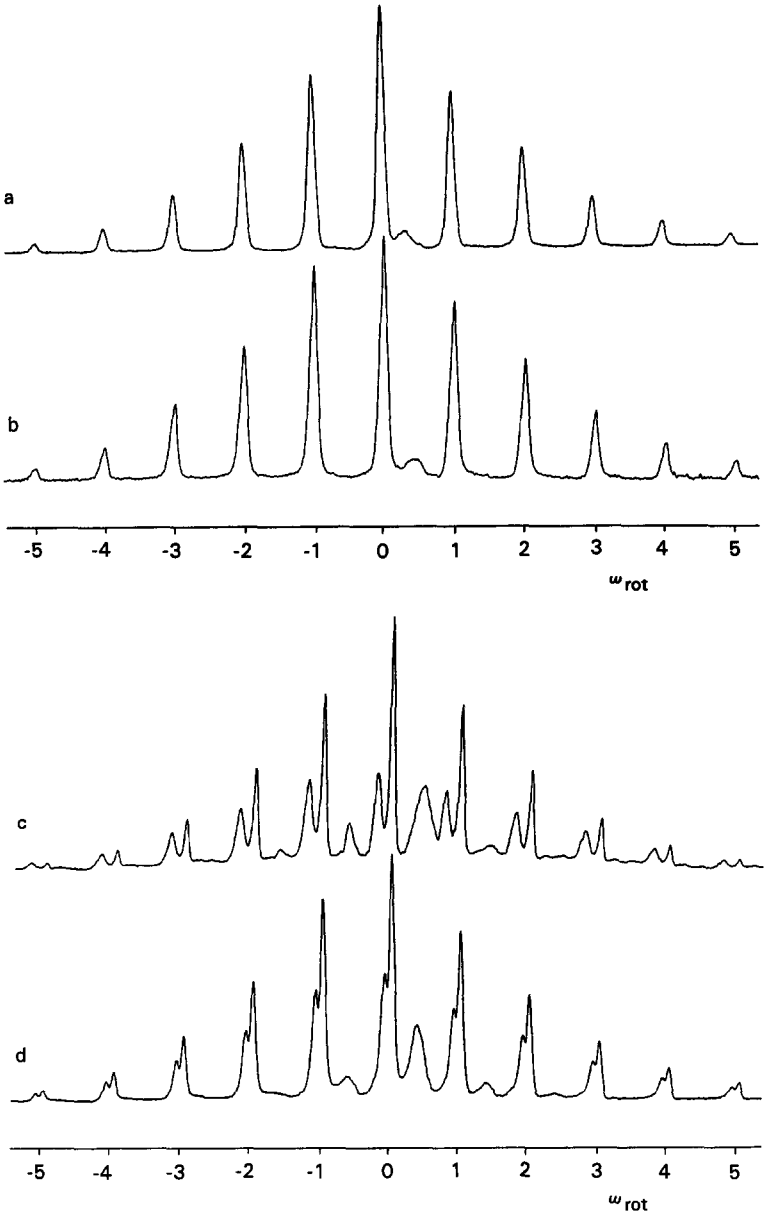

Fig 8 ^{1}H MAS NMR sideband pattern of the SAPO-34 recorded at a resonance frequency of 300 MHz (a) and 400 MHz (b), and of the SAPO-5 (c) and SAPO-37 (d) recorded at 400 MHz (* MAS sidebands)

oxygens must be larger than 2 5 ms which excludes restrictions for the magnetization transfer due to thermal motions of the hydroxyl protons Hence, the ^{29}Si CP/MAS NMR is suitable to yield information concerning the atoms in the second coordination sphere of the T positions of the bridging OH groups by the study of the enhancement of the various ^{29}Si NMR lines corresponding to the Si(nAl) sites with $n=4$ to 1

In the ^{29}Si CP/MAS NMR spectrum of the calcined 25HNa-A zeolite (Fig 2c) the line at $-90\,2$ ppm corresponds to the Si(4Al) atoms

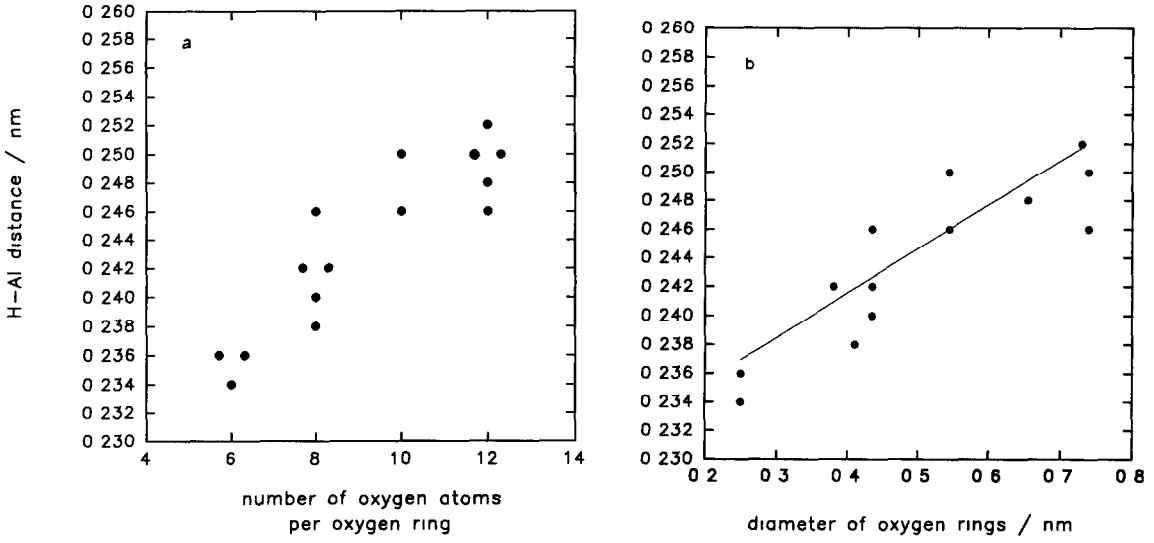

Fig 9 Plot of the experimentally determined H–Al distances r_{HAl} of bridging OH groups as a function of the number of oxygen atoms per oxygen ring (a) and of the diameters of the oxygen rings (b), using the values in Table 1 and 3

Because of the regularity of the LTA framework with a Si/Al ratio of 1 (Lowenstein rule) no other location of the hydroxyl protons as in the neighbourhood of Si(4Al) is possible The ^{29}Si MAS NMR spectrum of the 50HNa-X zeolite (Fig 2e) shows lines of the Si(4Al), Si(3Al) and Si(2Al) sites With cross-polarization, however, only the line of the Si(4Al) sites is enhanced (Fig 2f) While the ^{29}Si MAS NMR spectrum of the calcined 37HNaK-erionite (Fig 5h) comprises lines of the $Si_{T1}(n\text{Al})$ and $Si_{T2}(n\text{Al})$ sites with $n=3$, 2, 1, the CP experiment (Fig 5i) enhances mainly the line of the Si_{T1}(2Al) and/or Si_{T2}(3Al) sites caused by a preferential location of the bridging hydroxyl protons at these sites Hence, in the 50% ammonium exchanged zeolite X and the 37% ammonium exchanged erionite, the bridging OH groups prefer a location in the neighbourhood of the Si(nAl) sites with the largest possible number n of aluminium atoms in the second coordination sphere of the T atoms

The ^{29}Si CP/MAS NMR spectra of the calcined 52HNa-Y and 90HNa-Y zeolite (Figs 5c and 5f) consist of lines corresponding to Si(2Al), Si(1Al) and a small amount of Si(3Al) sites The variation of the framework Si/Al ratio from 2 4 to 5 0 causes a decrease of the number of Si(3Al) and Si(2Al) sites while the number of Si(1Al) sites increases [12] In the 52HNa-Y zeolite, which exhibit only O1H groups, as well as in the 90HNa-Y zeolite with a maximum number of O3H groups, these O1H and O3H groups are located in the neighbourhood of the Si(3Al) and Si(2Al) sites as well as the Si(1Al) sites Hence, if hydroxyl protons also prefer a siting at Si(nAl) with the largest possible number n, this causes in aluminosilicates with a medium framework aluminium density ($2\,43 < Si/Al < 5\,0$) a location of the bridging OH groups at the Si(nAl) sites with a wide range of numbers n (3, 2 and 1)

According to the ^{29}Si CP/MAS NMR spectra of the H-mordenite (Fig 5l) and the H-ZSM-5 zeolites (not shown) only the Si(1Al) sites are responsible for the formation of bridging OH groups The values of M_2^{ext} (see Table 3) are in agreement with the large distance of the bridging OH groups to the second-nearest framework aluminium nuclei and the absence of extra-framework aluminium species The ^{29}Si MAS NMR spectra of the silicoaluminophosphates (Figs 6a and 6c to 6e) and the CP/MAS spectrum of the calcined SAPO-5 (Fig 6b) show that for the silicoaluminophosphate type zeolites under study ($Si/(Al+P+Si) < 0\,12$) the incorporation of silicon into

the framework takes place mainly at the phosphorus positions producing isolated Si(4Al) sites Flanigen *et al* [27] suggested that the occurrence of either Si substituting for Al alone, or two Si for one Al and one P is unlikely in silicoaluminophosphates, since each of them creates Si–O–P linkages Moreover, because of the large electronegativity of phosphoros [32], the resonance position of the Si(*n*P, (4-*n*)Si) sites should be shifted to higher magnetic field Because of the strict alternation of aluminium and phosphorus tetrahedra in the parent aluminophosphate structure [15], the second coordination sphere of the T positions of each Si(4Al) site with respect to the bridging OH group is occupied by three aluminium atoms and three phosphorus atoms As can be seen from Table 3, the numerical ^{1}H MAS NMR sideband analysis yields a second moment $M_2^{ext} = 1\,1 \pm 0\,3\ 10^8\ s^{-2}$ for all bridging hydroxyl protons of the silicoaluminophosphates studied in the present paper Since all bridging OH groups exhibit an equal number of aluminium and phosphorus atoms in the second coordination sphere of the T atoms, the resulting magnetic dipole interactions give rise to a constant contribution to the second moment M_2^{ext} corresponding to the small fluctuation observed for this parameter (Table 3) comparing the various silicoaluminophosphates

Conclusions

The numerical analysis of the ^{1}H MAS NMR sideband pattern of the bridging OH groups in aluminosilicate and silicoaluminophosphate type zeolites yields H–Al distances r_{HAl} of the hydroxyl protons to the adjacent framework aluminium nuclei which cover a range between 0 234 and 0 252 nm From the results, a relation between the H–Al distance and the size of the oxygen rings (6-, 8-, 10- and 12-membered oxygen rings) could be derived The numerical analysis of the ^{1}H MAS NMR spectra recorded at different magnetic fields confirmed that the mathematical model described above is suitable to simulate the sideband pattern of the bridging OH groups in zeolites Using ^{29}Si CP/MAS NMR, it was shown that in zeolites of aluminosilicate type, the bridging OH groups prefer a location at the Si(*n*Al) sites with a maximum number *n* of aluminium atoms, while in zeolites of silicoaluminophosphate type with Si/(Al + P + Si) < 0 12 the second coordination sphere of the T positions with respect to the bridging OH group is always occupied by the same number of aluminium and phosphorus atoms The second moment M_2^{ext} of the magnetic dipole interaction of the hydroxyl protons with nuclei at distances much larger than r_{HAl}, determined by the numerical ^{1}H MAS NMR sideband analysis, correlates well with the number and kind of atoms in the second coordination sphere of the T positions

Acknowledgement

We thank Prof D Freude (Leipzig) and Dr G Engelhardt (Stuttgart) for helpful comments and Dr D Fenzke (Leipzig) for his assistance in the computer-aided sideband analysis Furthermore, we are grateful to Dr G Finger, Dr U Lohse and Mrs I Girnus (all in Berlin) for the preparation of the SAPO-5, SAPO-17 and SAPO-34, respectively

References

1 J Sauer, *J Mol Catal*, 54 (1989) 312
2 L A Curtiss, H Brand, J B Nicholas and L E Iton, *Chem Phys Lett*, 184 (1991) 215
3 K-P Schroder, J Sauer, M Leslie, C R A Catlow and J M Thomas, *Chem Phys Lett*, 188 (1992) 320
4 M Czjzek, H Jobic, A N Fitch and T Vogt, *J Phys Chem*, 96 (1992) 1535
5 R L Stevenson, *J Catal*, 21 (1971) 113
6 D Freude, J Klinowski and H Hamdan, *Chem Phys Lett*, 149 (1988) 355
7 D Fenzke, M Hunger and H Pfeifer, *J Magn Reson*, 95 (1991) 477
8 W Schwieger, K-H Bergk, D Freude, M Hunger and H Pfeifer, *ACS Symp Ser*, 398 (1989) 274
9 G Finger, J Kornatowski, J Richter-Mendau, K Jancke, M Bulow and M Rozwadowski, *Stud Surf Sci Catal*, 65 (1991) 501
10 B M Lok, C A Messina, R L Patton, R T Gajek, T R Cannan and E M Flanigen, *US Pat* 4400871 (1984)
11 A F Ojo, J Dwyer, J Dewing and K Karim, *J Chem Soc Faraday Trans*, 87 (1991) 2676
12 G Engelhardt and D Michel, *High-Resolution Solid-State*

NMR of Silicates and Zeolites, Wiley, Chichester, 1987, pp 154, 216 and 246
13 J J Pluth and J V Smith, *J Am Chem Soc*, 105 (1983) 1192
14 M Hunger, D Freude, T Frohlich and H Pfeifer, *Zeolites*, 7 (1987) 108
15 E M Flanigen, B M Lok, R L Patton and S T Wilson, *Pure Appl Chem*, 58 (1986) 1351
16 V M Mastikhin, I L Mudrakowsky and A V Nosov, *Progr Nucl Magn Reson Spectrosc*, 23 (1991) 259
17 M Hunger, D Freude, H Pfeifer, D Prager and W Reschetilowski, *Chem Phys Lett*, 163 (1989) 221
18 D Freude, M Hunger and H Pfeifer, *Z Phys Chem N F*, 152 (1987) 171
19 D Freude, M Hunger, H Pfeifer and W Schwieger, *Chem Phys Lett*, 128 (1986) 62
20 P A Jacobs and J B Uytterhoeven, *J Chem Soc Faraday Trans 1*, 69 (1973) 359
21 J W Ward, *ACS Monogr* 171 (1976) 145
22 H Ernst, Dissertation B, Department of Physics, University of Leipzig, 1988
23 K P Lillerud, *Zeolites*, 7 (1987) 14
24 C A Fyfe, G C Gobi, G J Kennedy, C T de Schutter, W J Murphy, R S Ozubko and D A Slack, *Chem Lett*, (1984) 163
25 D W Breck, *Zeolite Molecular Sieves*, Robert E Krieger Publishing Company, Malabar, FL, 1974, pp 65 and 636
26 A Kogelbauer, J A Lercher, K-H Steinberg, F Rossner, A Soellner and R V Dmitriev, *Zeolites*, 9 (1989) 224
27 E M Flanigen, R L Patton and S T Wilson, *Stud Surf Sci Catal*, 37 (1988) 13
28 F Rossner, K-H Steinberg, D Freude, M Hunger and H Pfeifer, *Stud Surf Sci Catal*, 46 (1989) 421
29 F Rossner, K-H Steinberg and S Rechenburg, *Zeolites*, 7 (1987) 488
30 B Zibrowius, E Loffler and M Hunger, *Zeolites*, 12 (1992) 167
31 D Freude, H Ernst, M Hunger, H Pfeifer and E Jahn, *Chem Phys Lett*, 143 (1988) 477
32 J Hocevar and B Drzaj, *J Catal*, 73 (1982) 27
33 T Bernstein, P Fink, V M Mastikhin and A A Shubin, *J Chem Soc Faraday Trans 1*, 82 (1986) 1879
34 M Hunger, E Loffler, U Lohse and B Zibrowius, in preparation
35 S Dzwigaj, M Briend, A Shikholeslami, M J Peltre and D Barthomeuf, *Zeolites*, 10 (1990) 157
36 D H Olson and E Dempsey, *J Catal*, 13 (1969) 221
37 H Rosenberger, R Zeiss and A-R Grimmer, *Z Chem*, 15 (1975) 162
38 D Heidemann, A-R Grimmer, P Starke, C Hubert and M Magi, *Z Anorg Allg Chem*, 37 (1985) 528
39 W M Meier and D H Olson, Atlas of Zeolite Structure Types, Butterworth-Heinemann, London, 1992
40 J V Smith, *Chem Rev*, 88 (1988) 149